

Contribution of Conserved Lysine Residues in the α_2 -Antiplasmin C Terminus to Plasmin Binding and Inhibition*

Received for publication, February 7, 2011, and in revised form, April 19, 2011. Published, JBC Papers in Press, May 4, 2011, DOI 10.1074/jbc.M111.229013

Bernadine G. C. Lu[†], Trifina Sofian[‡], Ruby H. P. Law[§], Paul B. Coughlin^{¶1}, and Anita J. Horvath^{†1,2}

From the [†]Australian Centre for Blood Diseases, Monash University, Melbourne, Victoria 3004, the [§]Department of Biochemistry and Molecular Biology, Monash University, Clayton, Victoria 3800, and the [¶]Department of Medicine and Haematology, Box Hill Hospital, Monash University, Box Hill, Victoria 3128, Australia

α_2 -Antiplasmin is the physiological inhibitor of plasmin and is unique in the serpin family due to N- and C-terminal extensions beyond its core domain. The C-terminal extension comprises 55 amino acids from Asn-410 to Lys-464, and the lysine residues (Lys-418, Lys-427, Lys-434, Lys-441, Lys-448, and Lys-464) within this region are important in mediating the initial interaction with kringle domains of plasmin. To understand the role of lysine residues within the C terminus of α_2 -antiplasmin, we systematically and sequentially mutated the C-terminal lysines, studied the effects on the rate of plasmin inhibition, and measured the binding affinity for plasmin via surface plasmon resonance. We determined that the C-terminal lysine (Lys-464) is individually most important in initiating binding to plasmin. Using two independent methods, we also showed that the conserved internal lysine residues play a major role mediating binding of the C terminus of α_2 -antiplasmin to kringle domains of plasmin and in accelerating the rate of interaction between α_2 -antiplasmin and plasmin. When the C terminus of α_2 -antiplasmin was removed, the binding affinity for active site-blocked plasmin remained high, suggesting additional exosite interactions between the serpin core and plasmin.

When tissue injury occurs, fibrinolysis and coagulation are activated in concert. Tissue plasminogen activator secreted by the injured endothelium activates plasminogen to plasmin, which in turn degrades the fibrin clot. Fibrinolysis remains localized because tissue plasminogen activator and plasminogen co-localize on fibrin strands, dramatically improving catalytic efficiency (1). In addition, free plasmin in plasma is rapidly inactivated by its principal regulator, α_2 -antiplasmin. Dysregulation of either fibrinolysis or coagulation has the potential to cause thrombosis, whereas on the other hand, therapeutic manipulation of these pathways can be used to treat thrombotic diseases (2). Currently, most therapeutic agents used to promote fibrinolysis directly activate plasminogen, but their use is limited by the risk of excessive bleeding. However, there is increasing evidence that α_2 -antiplasmin is a useful alternative target in the development of new therapeutics for thrombotic diseases (3).

α_2 -Antiplasmin is unique among the serpin family due to the presence of N- and C-terminal extensions beyond its inhibitory core. The 42-amino acid N terminus is cross-linked to fibrin by factor XIIIa, localizing its activity to the clot (4, 5). The α_2 -antiplasmin C terminus extends 55 amino acids from Asn-410 to Lys-464 and is believed to be important in the initial interaction with kringle domains of plasmin (6). A form of α_2 -antiplasmin that lacks the C terminus interacts with plasmin much more slowly compared with the intact molecule (7). The crystal structure of murine α_2 -antiplasmin lacking the first 43 amino acids has been determined; however, the C terminus could not be modeled, which suggests that the C-terminal region of α_2 -antiplasmin is highly flexible (8).

The C terminus of α_2 -antiplasmin contains six lysines, five of which are conserved between species (Lys-427, Lys-434, Lys-441, Lys-448, and Lys-464), and it is known that lysines are key in mediating binding to kringle domains. Using a synthetic peptide corresponding to the final 26 amino acids of the C terminus, a previous study showed that the α_2 -antiplasmin/plasmin association was reduced, indicating that this region has high affinity for plasmin kringle domains (9). However, the relative importance assigned to the C-terminal lysine compared with other internal lysines differs in published studies. Frank *et al.* (6) and Gerber *et al.* (10) studied the binding of kringle domains to C-terminal peptide containing Lys-to-Ala mutations. They showed that the C-terminal lysine (Lys-464) was the most important contributor to binding affinity for plasmin kringle domains (6, 10). However, kinetic inhibitory studies by Wang *et al.* (11) indicated that Lys-448 in full-length α_2 -antiplasmin was most important in the interaction with plasmin.

At present, there are no comprehensive studies investigating the role of lysine residues using inhibitory rates as an end point. To fully understand the role of the C-terminal lysine residues in the interaction with kringle domains of plasmin, we present a systematic and sequential study on the mutagenesis of α_2 -antiplasmin C-terminal lysines (Lys-427, Lys-434, Lys-441, Lys-448, and Lys-464) and truncation of the C terminus. This is the first report describing the plasmin inhibition rate (k_a) for full-length human α_2 -antiplasmin and intact plasmin. Furthermore, we investigated the binding affinity (K_D) of wild-type α_2 -antiplasmin and various mutants for active site-blocked plasmin using plasmon surface resonance. These studies suggest additional exosite interactions between the serpin core domain and plasmin.

* This work was supported by the National Health and Medical Research Council (NHMRC) of Australia.

[†] Both authors contributed equally to this work.

² To whom correspondence should be addressed: Australian Centre for Blood Diseases, Level 6 Burnet Bldg., 89 Commercial Rd., Melbourne, Victoria 3004, Australia. E-mail: anita.horvath@monash.edu.

EXPERIMENTAL PROCEDURES

Construction of α_2 -Antiplasmin Variants—Human WT α_2 -antiplasmin cDNA was isolated from a liver cDNA library using PCR with primers 5'-GGA TCC ACC CCA GGA GCA GGT GTC CC-3' and 5'-GGA TCC TCA CTT GGG GCT GCC AAA C-3'. The product was cloned into the pET-His(3a) expression vector and sequenced for authenticity (12). The QuikChange site-directed mutagenesis kit (Stratagene) was used on human WT α_2 -antiplasmin template in which alanine or stop codons were introduced at various lysine residues along the C terminus. Several mutations within the C terminus of human α_2 -antiplasmin were made as follows: K427A, K434A, K441A, K448A, K464A, P414stop (Cterm Δ), K448A/K464A, K434A/K448A/K464A, K434A/K441A/K448A/K464A, K427A/K434A/K441A/K448A/K464WT, L449stop, and K448A/L449stop (see Fig. 1).³ All constructs were nucleotide-sequenced to confirm the mutations introduced.

Expression and Purification of α_2 -Antiplasmin Variants—Recombinant human α_2 -antiplasmin (WT and mutants) was expressed in *Escherichia coli* BL21(DE3)pLysS cells. Cells were grown overnight at 37 °C with shaking at 220 rpm in 2 \times tryptone-yeast culture medium supplemented with 50 μ g/ml ampicillin. The cell cultures were then diluted 1:10 in fresh 2 \times tryptone-yeast medium supplemented with 50 μ g/ml ampicillin and grown for a further 2 h at 37 °C and 220 rpm. Human α_2 -antiplasmin was then induced with a final concentration of 0.02 mM isopropyl β -D-thiogalactopyranoside and incubated for 4 h at 30 °C and 220 rpm. Cells were harvested by centrifugation at 3500 rpm (Beckman JS-4.2 rotor) for 20 min and stored at -80 °C until used.

To obtain soluble recombinant α_2 -antiplasmin, the cell pellet was lysed in lysis buffer (50 mM NaPO₄ (pH 8.0), 500 mM NaCl, 20 mM imidazole, and 5 mM β -mercaptoethanol) containing 1 mg/ml lysozyme, 0.2 mg/ml DNase, 1:1000 protease inhibitor mixture (Sigma), and 0.01% phenylmethanesulfonyl fluoride per liter of cell culture. The cells were frozen in liquid nitrogen and then completely thawed three times in a 37 °C water bath. The lysate was centrifuged (Sorvall SS34 rotor) at 18,000 rpm for 20 min. To purify recombinant α_2 -antiplasmin, the supernatants were loaded onto a HisTrap column (GE Healthcare) and eluted with a linear imidazole gradient (0.02–0.5 M) in lysis buffer. The proteins were further purified on a Mono Q column (GE Healthcare) with a linear NaCl gradient (0–0.5 M) in 20 mM Tris (pH 8.0) and 0.1 mM EDTA. All recombinant human α_2 -antiplasmin was electrophoresed on 12.5% SDS-polyacrylamide gel to confirm the purity of peak fractions. Aliquots of recombinant protein were stored at -80 °C until used.

Determination of Stoichiometry of Inhibition—The stoichiometry of inhibition (SI)⁴ was determined by incubating 1 nM human plasmin (Hematologic Technologies, Essex Junction, VT) with WT α_2 -antiplasmin and mutants at various concentrations (0.2–1.5 nM) for 1 h at 37 °C. Residual plasmin activity was assayed at 25 °C using a FLUOstar Optima plate reader

(BMG Labtech, Victoria, Australia) set at 355/460 nm with 200 μ M fluorogenic substrate *H*-Ala-Phe-Lys-AMC (Bachem, Bubendorf, Switzerland). All reactions were done in triplicates in 20 mM Tris (pH 8.0), 150 mM NaCl, and 0.01% Tween 80 in a 1% bovine serum albumin-coated PerkinElmer OptiPlate.

Measuring the Rate of Plasmin Inhibition via Kinetic Assay—The rate of plasmin inhibition by recombinant α_2 -antiplasmin was determined using a continuous method described previously (13). Plasmin (0.5 nM) was reacted with various concentrations of recombinant α_2 -antiplasmin, WT (1.0–2.5 nM) or mutant (1.5–40 nM), in the presence of 1 mM *H*-Ala-Phe-Lys-AMC at 25 °C. Fluorescence emission was continuously measured using a FLUOstar Optima plate reader at 355/460 nm over time. Triplicate experiments were performed with each recombinant α_2 -antiplasmin in 20 mM Tris (pH 8.0), 150 mM NaCl, and 0.01% Tween 20 in a 1% bovine serum albumin-coated PerkinElmer OptiPlate.

The raw data were fitted using nonlinear regression in GraphPad Prism (Equation 1),

$$P = \frac{V_0}{k_{\text{obs}}} \times (1 - e^{(-k_{\text{obs}}t)}) \quad (\text{Eq. 1})$$

where P is the concentration of product at time t , V_0 is the initial velocity, and k_{obs} is the apparent first-order rate constant (14). The k_{obs} value for each serpin concentration was calculated by Equation 1. Each k_{obs} value was plotted against the respective α_2 -antiplasmin concentration. Linear regression analysis was performed to obtain the uncorrected rate of inhibition (k'). Equation 2 was used to account for fluorogenic substrate competition,

$$k_a = k' \times \left(1 + \frac{[S]}{K_m}\right) \times \text{SI} \quad (\text{Eq. 2})$$

where the rate of inhibition was adjusted with the SI, substrate concentration ($[S]$), and Michaelis constant (K_m) of the substrate to give the second-order rate constant (k_a) (14).

Binding of α_2 -Antiplasmin to Active Site-blocked Plasmin by Surface Plasmon Resonance—The interactions between active site-blocked plasmin and various recombinant α_2 -antiplasmin proteins were determined via surface plasmon resonance using the Biacore T100 system (GE Healthcare). Active site-blocked plasmin was produced by incubating human plasmin with a 1000-fold molar excess of D-Val-Phe-Lys chloromethyl ketone (Calbiochem) at 37 °C for 1 h. Active site-blocked plasmin was then dialyzed overnight at 4 °C in running buffer (0.01 M HEPES (pH 7.4), 0.15 M NaCl, 50 μ M EDTA, and 0.05% surfactant P20 (GE Healthcare)). To confirm that the active site was completely blocked, the activity of active site-blocked plasmin was checked against active plasmin in the presence of 200 μ M *H*-Ala-Phe-Lys-AMC fluorogenic substrate.

To measure the binding affinity and rate of plasmin association of α_2 -antiplasmin with active site-blocked plasmin, we immobilized hexahistidine-tagged WT or mutant α_2 -antiplasmin on the nitrilotriacetic acid (NTA) surface of a NTA chip (GE Healthcare) following the manufacturer's instructions. All experiments were carried out in running buffer at a flow rate of 10 μ l/min and performed in triplicates. Briefly, the NTA sur-

³ The numbering of recombinant α_2 -antiplasmin variants was based on the secreted 464-residue form (5).

⁴ The abbreviations used are: SI, stoichiometry of inhibition; AMC, 7-amino-4-methylcoumarin; NTA, nitrilotriacetic acid.

α_2 -Antiplasmin Binding to Plasmin

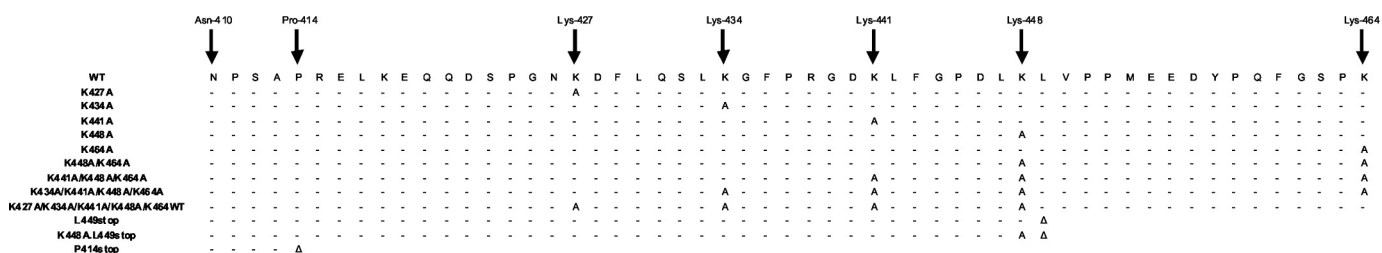


FIGURE 1. Schematic representation of the C terminus of α_2 -antiplasmin and positions at which mutations were introduced. Full-length WT α_2 -antiplasmin and various mutants (Lys-to-Ala mutations or truncation) of the C terminus were generated, expressed, and purified. Dashes represent the wild-type sequence, and the introduction of a stop codon is indicated (Δ).

face was activated by injecting 500 μM NiCl_2 for 1 min. 20 nM WT or mutant recombinant α_2 -antiplasmin was immobilized onto the surface on one flow cell for 1 min. A reference flow cell containing no α_2 -antiplasmin was used to account for nonspecific binding to the NTA surface. Six different concentrations of active site-blocked plasmin (analyte) were injected for 1 min of association time, followed by 10 min of dissociation time. The range of active site-blocked plasmin concentrations (2–120 nM) was adjusted for each α_2 -antiplasmin variant. At the end of each concentration cycle, the NTA surface was completely stripped with regeneration buffer (0.01 M HEPES (pH 7.4), 0.15 M NaCl, 0.35 M EDTA, and 0.05% surfactant P20) at a flow rate of 30 $\mu\text{l}/\text{min}$ for 2 min. NTA surface activation and α_2 -antiplasmin immobilization were performed at each active site-blocked plasmin concentration. The injection needle was cleaned with an extra wash of running buffer after each subsequent step.

Real-time binding curves were monitored on a sensorgram as resonance units over time. For kinetic and binding affinity analysis of recombinant α_2 -antiplasmin with active site-blocked plasmin, we used the two-state reaction model provided in the Biacore T100 evaluation software (Version 1.1.1) (Equation 3).

$$E + I \rightleftharpoons EI \rightleftharpoons EI^* \quad (\text{Eq. 3})$$

This model describes a 1:1 binding of analyte to immobilized ligand, followed by a secondary interaction that stabilizes the two molecules. χ^2 analysis supported this model. The overall equilibrium dissociation constant (K_D) was calculated using Equation 4 (15).

$$K_D = \frac{k_{d1}}{k_{a1}} \times \frac{k_{d2}}{k_{d2} + k_{a2}} \quad (\text{Eq. 4})$$

RESULTS

Stoichiometry of Inhibition between Recombinant Human α_2 -Antiplasmin and Plasmin—To examine the role of lysine residues in the α_2 -antiplasmin C terminus, we employed site-directed mutagenesis and produced a series of mutant recombinant proteins (Fig. 1). Mutations within the C-terminal region of α_2 -antiplasmin would not be expected to affect the inhibitory mechanism because this property resides in the serpin core domain. However, to verify that the recombinant proteins were correctly folded, the SI for human plasmin was determined for WT and mutant α_2 -antiplasmin.

The serpin/protease ratio that resulted in complete loss of protease activity was determined as the SI of the serpin (Fig. 2). The SI of WT α_2 -antiplasmin was found to be 1.0 (Fig. 2, A and

E) and corresponds with published values (16). Fig. 2E shows the SI values obtained for each recombinant protein produced. All mutants were shown to have an SI of between 0.9 and 1.5 (Fig. 2, B–E), indicating that the efficiency of mutant protein had not been structurally perturbed by the introduction of various amino acid substitutions in the C terminus. To confirm these observations, WT recombinant α_2 -antiplasmin and mutants were also assessed by CD spectrometry. Mutant α_2 -antiplasmin proteins produced CD spectra similar to WT α_2 -antiplasmin, demonstrating that the mutant proteins retained their native fold (data not shown).

Rate of Plasmin Inhibition of Recombinant Human α_2 -Antiplasmin Variants—The primary hypothesis being tested in this work is that lysine residues at the extreme C terminus of α_2 -antiplasmin as well as internally within the C-terminal extension accelerate inhibition of plasmin. Therefore, kinetic studies using a protease inhibition (progress curve) assay were performed to measure the rate of plasmin inhibition by WT and mutant α_2 -antiplasmin. Fig. 3 shows examples of progress and fitted curves obtained from the analysis of WT and P414stop (Cterm Δ) α_2 -antiplasmin.

As expected, recombinant human WT α_2 -antiplasmin was a fast inhibitor of human plasmin, with a plasmin inhibition rate (k_a) of $(3.7 \pm 0.3) \times 10^7 \text{ M}^{-1} \text{ s}^{-1}$, which corresponds to published results (17). Individual Lys-to-Ala mutations at positions 427, 434, 441, 448, and 464 caused decreases in the rate of plasmin inhibition of 1.5-, 1.6-, 1.7-, 2.8-, and 3.6-fold respectively (Fig. 4) compared with WT α_2 -antiplasmin. The K464A mutation produced the greatest reduction in the rate of plasmin inhibition; however, this was modest compared with the effect of removing the entire α_2 -antiplasmin C terminus (P414stop), which resulted in a 40-fold reduction ($k_a = (9.2 \pm 0.2) \times 10^5 \text{ M}^{-1} \text{ s}^{-1}$).

Because the reductions in the inhibition rate observed with individual Lys-to-Ala mutants were small compared with the effect of removal of the complete C terminus, we examined the effect of progressive mutations of the Lys residues in this domain. Compared with α_2 -antiplasmin K464A, each additional mutation (K448A/K464A, K441A/K448A/K464A, and K434A/K441A/K448A/K464A) resulted in an \sim 2-fold reduction in the plasmin inhibition rate (Fig. 5). Therefore, the overall reduction in the rate of plasmin inhibition observed with the four-residue substitution (K434A/K441A/K448A/K464A) was 45-fold, which is comparable with the effect of removing the entire α_2 -antiplasmin C terminus (P414stop).

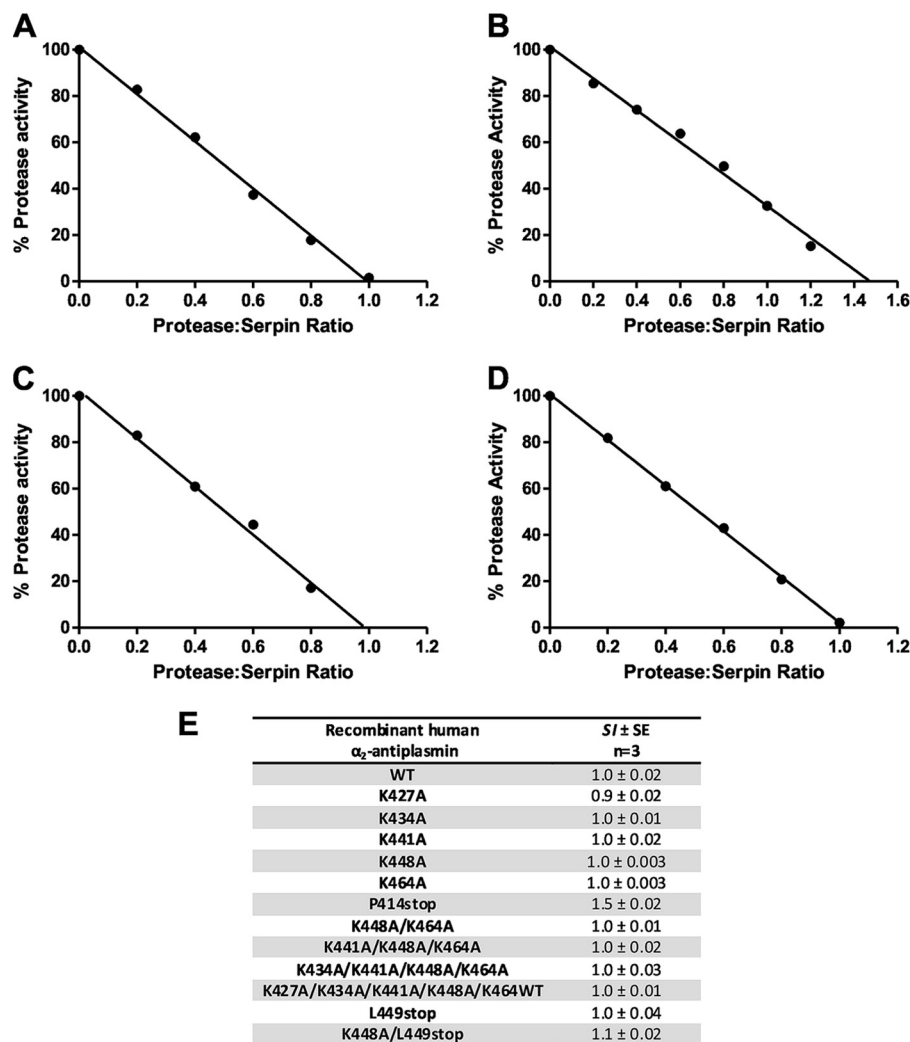


FIGURE 2. SI of plasmin by recombinant human α_2 -antiplasmin. Plasmin (1 nM) was incubated with WT or mutant α_2 -antiplasmin (0.2–1.5 nM) for 1 h at 37 °C. Residual protease activity was measured in the presence of H-Ala-Phe-Lys-AMC (0.2 mM). A, WT recombinant α_2 -antiplasmin; B, P414stop (Cterm Δ) mutant α_2 -antiplasmin; C, K464A mutant α_2 -antiplasmin; D, K434A/K441A/K448A/K464A mutant α_2 -antiplasmin; E, mean SI of plasmin by WT and mutant recombinant α_2 -antiplasmin.

It is conceivable that substitution of four lysine residues within the C terminus of α_2 -antiplasmin could produce a structural perturbation of the domain. We therefore measured the kinetic effect of adding the lysine analog ϵ -aminocaproic acid to the inhibitory reaction. When 1 mM ϵ -aminocaproic acid was added to the inhibitory reaction, a k_a of $(2.3 \pm 0.2) \times 10^6 \text{ M}^{-1} \text{ s}^{-1}$ was observed, which was comparable with the mutant with a deletion of the C terminus (P414stop) ($k_a = (9.2 \pm 0.2) \times 10^5 \text{ M}^{-1} \text{ s}^{-1}$) (Fig. 4). This suggests that most of the reduction in the plasmin inhibition rate caused by the removal of the C terminus can be accounted for by lysine-specific interactions.

The relative importance of the C-terminal Lys-464 compared with the internal lysine residues was further addressed by measuring the rate of inhibition of a mutant in which Lys-464 was preserved while the internal lysines were mutated to alanine (K427A/K434A/K441A/K448A/K464A) (Fig. 5). This mutant demonstrated a 5.2-fold rate reduction ($k_a = (7.1 \pm 0.1) \times 10^6 \text{ M}^{-1} \text{ s}^{-1}$) compared with WT α_2 -antiplasmin.

The importance of the C-terminal lysine was further evaluated by producing a mutant in which a stop codon was intro-

duced after Lys-448 (L449stop). Despite this mutant possessing a C-terminal lysine, it still showed a rate reduction in plasmin inhibition ($k_a = (1.1 \pm 0.1) \times 10^5 \text{ M}^{-1} \text{ s}^{-1}$) of 3.4-fold compared with WT α_2 -antiplasmin. Additionally, when the L449stop mutant was modified by substituting Lys-448 with Ala (K448A/L449stop), there was a further decrease in the plasmin inhibition rate ($k_a = (2.8 \pm 0.1) \times 10^6 \text{ M}^{-1} \text{ s}^{-1}$).

Binding Affinity of Recombinant Human α_2 -Antiplasmin Variants for Active Site-blocked Plasmin—The association rate constants described above were derived from measurements of inhibition of plasmin amidolytic activity. To corroborate these results and to partition the α_2 -antiplasmin/plasmin interaction between the serpin core versus the C-terminal extension, we used surface plasmon resonance to directly measure the binding affinity of recombinant human α_2 -antiplasmin for human plasmin. WT α_2 -antiplasmin and various mutants were reacted with active site-blocked plasmin, and binding was observed in real time. The association and dissociation constants were calculated to obtain the binding affinity (K_D). Examples of sensorgrams for the interaction between active site-blocked plasmin

α_2 -Antiplasmin Binding to Plasmin

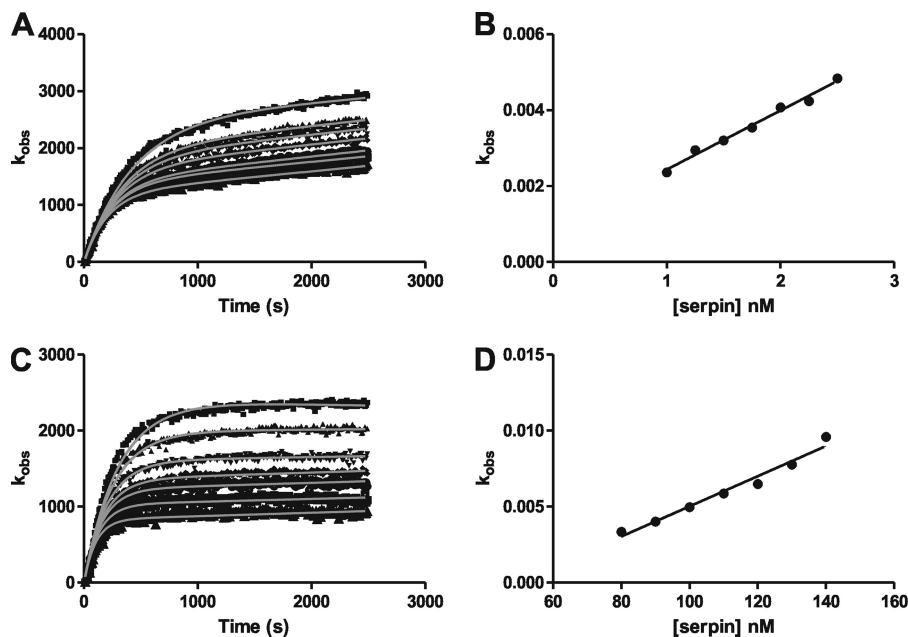


FIGURE 3. **Plasmin inhibition by recombinant human α_2 -antiplasmin.** A, progress curves of plasmin inhibition using plasmin (0.5 nM) and WT α_2 -antiplasmin (1–2.5 nM) in the presence of H-Ala-Phe-Lys-AMC (1 mM). Nonlinear regression analysis using Equation 1 was used to determine the first-order rate constant (k_{obs}). B, the k_{obs} is plotted against the WT α_2 -antiplasmin concentration, and linear regression analysis was performed to determine the uncorrected second-order rate constant (k'). To account for substrate inhibition, Equation 2 was applied to determine the corrected second-order rate constant (k_a). C, progress curves of plasmin inhibition using plasmin (0.5 nM) and P414stop (Cterm Δ) α_2 -antiplasmin (80–140 nM) in the presence of H-Ala-Phe-Lys-AMC (1 mM). The k_{obs} was obtained as described above. D, the k_{obs} is plotted against the Cterm Δ α_2 -antiplasmin concentration to determine the k' . The k_a of Cterm Δ α_2 -antiplasmin was calculated using Equation 2.

and recombinant α_2 -antiplasmin are shown in Fig. 6. To achieve similar response units for WT α_2 -antiplasmin (Fig. 6A), a higher concentration of active site-blocked plasmin was used with α_2 -antiplasmin mutants, which accounts for the difference in the shape of the binding curves observed in the sensorgrams (Fig. 6).

The K_D of WT α_2 -antiplasmin for active site-blocked plasmin was determined to be 1.6 nM, indicating a high affinity interaction. Single Lys-to-Ala mutants at positions 448 and 464 showed decreases in K_D of 1.3- and 3.3-fold, respectively (Fig. 7), compared with WT α_2 -antiplasmin. Removing the C terminus (P414stop) resulted in a 31-fold reduction in K_D (50 nM). Overall measurements of binding affinity were consistent with association rates observed using the progress curve plasmin inhibition assay.

Sequential mutation of the Lys residues within the C terminus resulted in a progressive decrease in the K_D , which corresponds to the observations made previously. K448A/K464A showed a 2.0-fold reduction in the K_D (10 nM) compared with K464A. K441A/K448A/K464A produced a 2.8-fold decrease compared with K448A/K464A. An additional 1.5-fold reduction in K_D was observed with K434A/K441A/K448A/K464A ($K_D = 42$ nM). The K_D for K434A/K441A/K448A/K464A was similar to that obtained by removing the C terminus of α_2 -antiplasmin (P414stop). The K_D for K427A/K434A/K441A/K448A/K464A was 13 nM, corresponding to a 8.4-fold decrease compared with WT α_2 -antiplasmin.

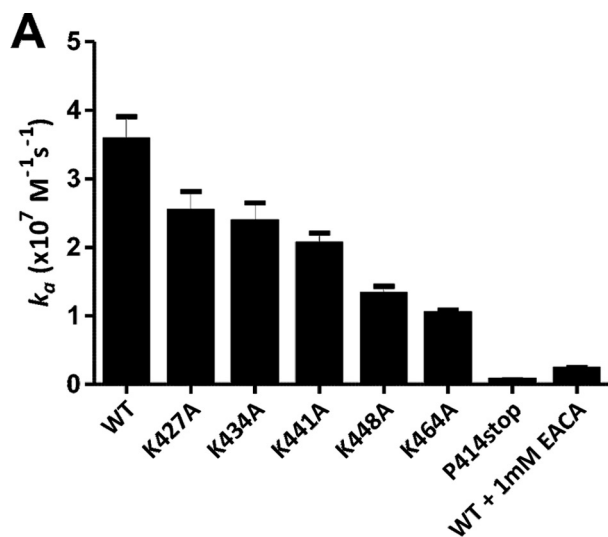
The L449stop mutant demonstrated a K_D of 6.4 nM, which is similar to that obtained for K464A ($K_D = 5.2$ nM). This further confirms what was seen previously with the rate of plasmin inhibition. Subsequent mutation of L449stop to K448A/

L449stop resulted in a 17-fold reduction in K_D (27 nM) compared with WT α_2 -antiplasmin.

The rate of plasmin association (k_{a1}) obtained using surface plasmon resonance was very similar to the rate of plasmin inhibition (k_a) obtained using the kinetic assay described previously. The dissociation rate constant (k_{d1}) and the forward and reverse rate constants (k_{a2} and k_{d2}) remained relatively unchanged for WT α_2 -antiplasmin and mutants with active site-blocked plasmin.

DISCUSSION

In this work, we have reported the first comprehensive description of the kinetics of α_2 -antiplasmin/plasmin interactions employing two different methods. By incorporating a fluorogenic substrate with high affinity for plasmin, we have been able to use the “progress curve” method to accurately measure the association rates for WT α_2 -antiplasmin and mutants. In addition, we have independently observed the α_2 -antiplasmin/plasmin interaction via surface plasmon resonance. In both methods, we employed full-length α_2 -antiplasmin (WT and mutants) and intact plasmin containing the pro-tease and all kringle domains. It is important to recognize that the two methods measure different kinetic rate constants. Using Fig. 8 as a reference schematic, surface plasmon resonance measures the initial rate of interaction (k_1) between α_2 -antiplasmin and plasmin. The protease inhibition assay (progress curve) measures the overall rate at which the irreversible covalent α_2 -antiplasmin·plasmin complex is formed, resulting in complete inhibition; therefore, this takes into account k_1 , k_2 , and k_4 (Fig. 8). We were able to obtain comparable rates of plasmin inhibition (k_a) and asso-

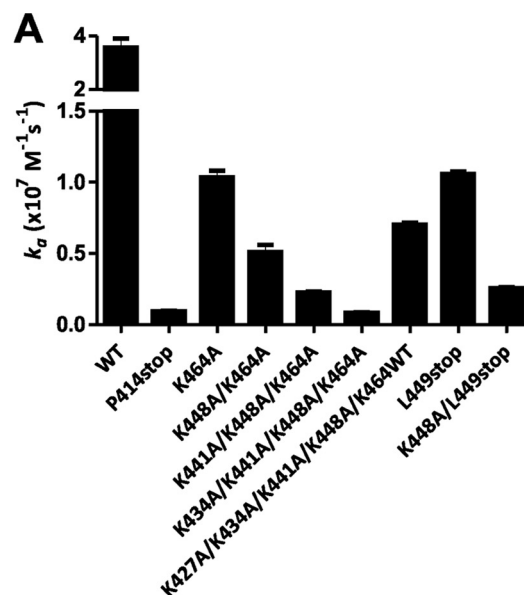


Recombinant human α_2 -antiplasmin	$k_a \pm SE$ ($M^{-1}s^{-1}$) n=3
WT	$3.7 \pm 0.3 \times 10^7$
K427A	$2.4 \pm 0.3 \times 10^7$
K434A	$2.3 \pm 0.3 \times 10^7$
K441A	$2.1 \pm 0.2 \times 10^7$
K448A	$1.3 \pm 0.1 \times 10^7$
K464A	$1.0 \pm 0.1 \times 10^7$
P414stop	$9.2 \pm 0.2 \times 10^5$
WT with 1mM EACA	$2.3 \pm 0.2 \times 10^6$ (n=2)

FIGURE 4. Effect of single Lys-to-Ala mutations in the human α_2 -antiplasmin C terminus on plasmin inhibition. A, mean rate of plasmin inhibition (k_a) by WT and mutant recombinant α_2 -antiplasmin ($n = 3$). B, mean k_a of plasmin for WT and mutant recombinant α_2 -antiplasmin.

ciation (k_{a1}) despite the fact that both methods measure different values. This indicates that the rapid interaction is predominantly due to the formation of the initial reversible encounter α_2 -antiplasmin-plasmin complex, thus suggesting that the rate-limiting step occurs when the covalent α_2 -antiplasmin-plasmin complex is formed.

Using protease inhibition and binding affinity data, we were able to demonstrate a progressive decrease in the rate of plasmin association, inhibition, and binding affinity with consecutive Lys-to-Ala mutations within the C terminus of α_2 -antiplasmin. We showed that all conserved Lys residues (Lys-427, Lys-434, Lys-441, Lys-448, and Lys-464) play a role in the interaction with kringle domains of plasmin, with Lys-464 being the main initiator, followed by Lys-448, which corresponds with previously published data (6, 10). Individually, the internal Lys residues appear to have a minor function in the interaction with plasmin. However, as demonstrated by several of our α_2 -antiplasmin mutants, primarily K434A/K441A/K448A/K464A and P414stop, we were able to show that when five of the lysines were mutated, the rates of plasmin inhibition and binding were reduced to those of the C-terminally truncated α_2 -antiplasmin protein. This indicates that the Lys residues within the C terminus of α_2 -antiplasmin are the primary mediators in the binding to the kringle domains and that removal of these



Recombinant Human α_2 -antiplasmin	$k_a \pm SE$ ($M^{-1}s^{-1}$) n=3
WT	$3.7 \pm 0.3 \times 10^7$
P414stop	$9.2 \pm 0.2 \times 10^5$
K464A	$1.0 \pm 0.1 \times 10^7$
K448A/K464A	$4.9 \pm 0.5 \times 10^6$
K441A/K448A/K464A	$2.2 \pm 0.1 \times 10^6$
K434A/K441A/K448A/K464A	$8.2 \pm 0.5 \times 10^5$
K427A/K434A/K441A/K448A/K464A	$7.1 \pm 0.1 \times 10^6$
L449stop	$1.1 \pm 0.1 \times 10^7$
K448A/L449stop	$2.8 \pm 0.1 \times 10^6$

FIGURE 5. Effect of sequential Lys-to-Ala mutations and truncations on the human α_2 -antiplasmin C terminus on plasmin inhibition. A, mean rate of plasmin inhibition (k_a) by WT and mutant recombinant α_2 -antiplasmin ($n = 3$). B, mean k_a of plasmin for WT and mutant recombinant α_2 -antiplasmin.

residues will result in the loss of C-terminal binding. Furthermore, K427A/K434A/K441A/K448A/K464A demonstrated that even with the presence of the most C-terminal lysine with all the internal lysines mutated, the plasmin inhibition rate obtained was not comparable with WT α_2 -antiplasmin. Therefore, each conserved Lys in the α_2 -antiplasmin C terminus participates in the binding and inhibition of plasmin.

Previous studies by Frank *et al.* (6) using individual recombinant plasmin kringle domains (K1, K3, K3mut, K4, and K5) showed that the isolated α_2 -antiplasmin C terminus had the highest affinity for K1, followed by K4, K5, and K2. In further experiments, Gerber *et al.* (10) examined the affinity of the recombinant plasmin kringle domains (K1, K1-3, K4, and K4-5). They demonstrated that progressive mutations of lysine residues within the α_2 -antiplasmin C terminus decreased the affinity for K1-3, although the greatest contribution to binding was attributable to Lys-464 and Lys-448. The apparent lack of effect on the affinity of mutations of Lys-418, Lys-427, Lys-434, and Lys-441 may be explained by the fact that only two lysine-binding kringle domains were present in the K1-3 protein. The seeming discrepancy between our results and those of Gerber *et al.* can therefore be

α_2 -Antiplasmin Binding to Plasmin

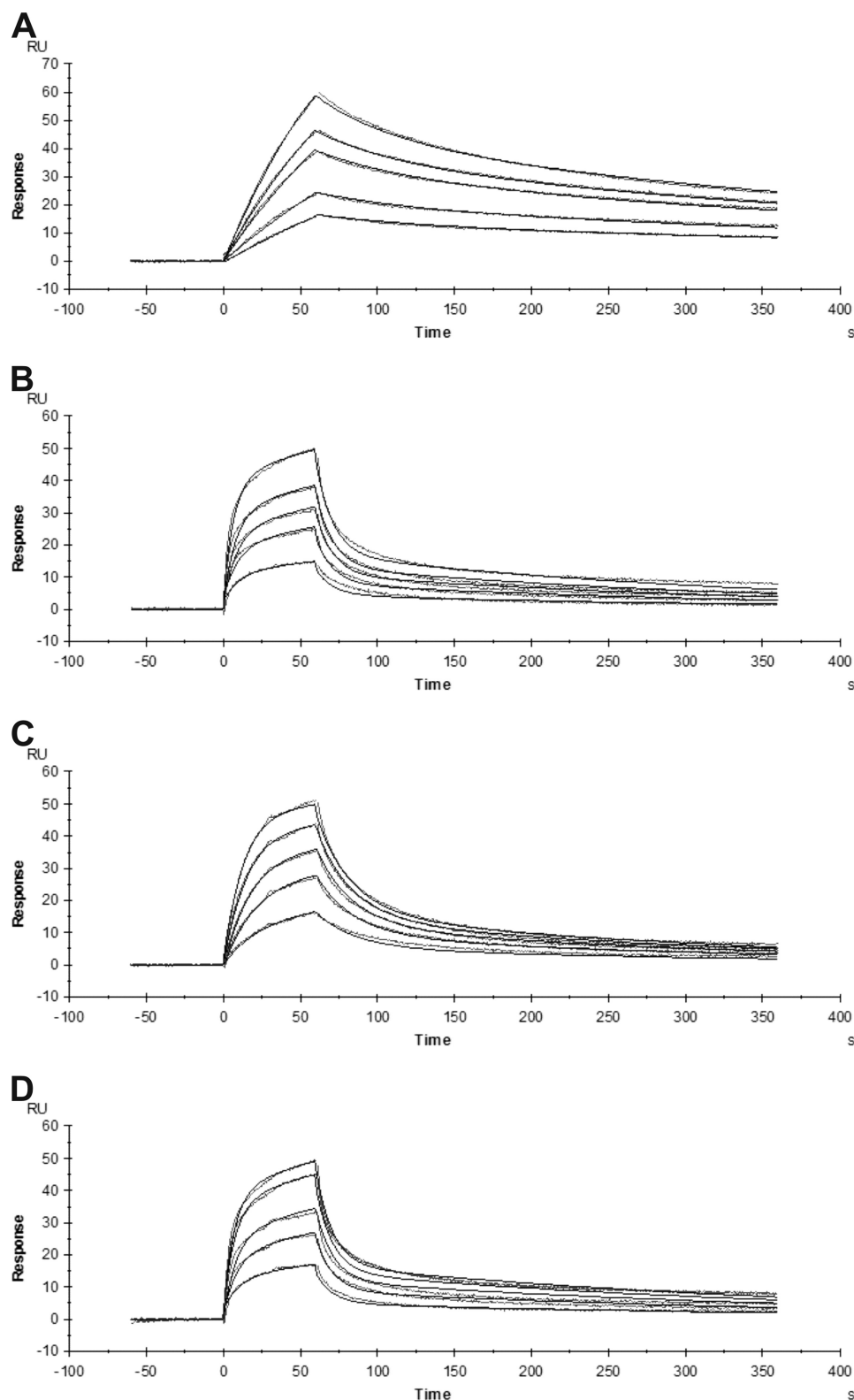


FIGURE 6. Sensorgrams of the binding of recombinant human α_2 -antiplasmin to active site-blocked plasmin measured by surface plasmon resonance. WT or mutant recombinant α_2 -antiplasmin (20 nM) was immobilized on a NTA chip. The binding of various concentrations of active site-blocked plasmin to α_2 -antiplasmin was monitored in real time. *A*, binding of active site-blocked plasmin (2–8 nM) to WT α_2 -antiplasmin ($\chi^2 = 0.21$). *B*, binding of active site-blocked plasmin (20–120 nM) to P414stop (Cterm Δ) recombinant α_2 -antiplasmin ($\chi^2 = 0.60$). *C*, binding of active site-blocked plasmin (4–20 nM) to K464A mutant α_2 -antiplasmin ($\chi^2 = 0.31$). *D*, binding of active site-blocked plasmin (20–100 nM) to K434A/K441A/K448A/K464A mutant α_2 -antiplasmin ($\chi^2 = 0.54$).

accounted for by differences in experimental approaches. They measured the association constants of isolated kringle domains (K1, K4, K1-3, and K4-5) with the C-terminal por-

tion of α_2 -antiplasmin. By contrast, this study describes the rate of plasmin inhibition and binding affinity of full-length α_2 -antiplasmin with intact plasmin.

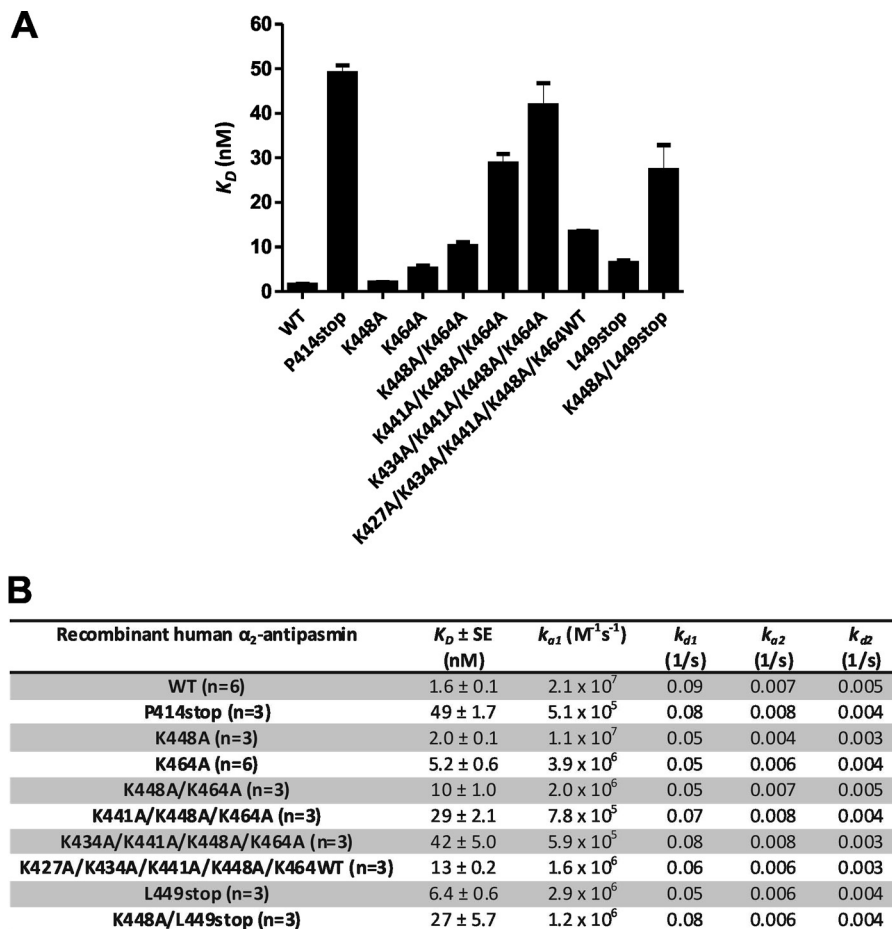


FIGURE 7. Effect of mutations in the α_2 -antiplasmin C terminus on binding to active site-blocked plasmin as studied via surface plasmon resonance. A, mean binding affinity (K_D) of WT and mutant recombinant α_2 -antiplasmin for active site-blocked plasmin ($n = 3$). B, mean K_D and association and dissociation constants of WT and mutant recombinant α_2 -antiplasmin for active site-blocked plasmin.

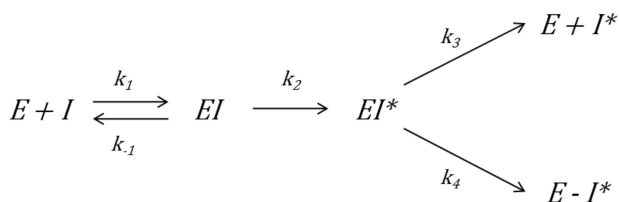


FIGURE 8. Mechanism of serpin inhibition. I represents serpin, and E represents the protease. The forward rate constant of serpin with protease is represented as k_1 . The association rate constant (k_{a1}) measured in surface plasmon resonance studies is equal to k_1 . k_{-1} is the reverse rate constant. The rate at which conformational change (EI^*) occurs is denoted as k_2 . k_3 occurs during the substrate reaction, which results in cleaved serpin and release of active protease ($E + I^*$). Formation of the covalent protease-serpin complex ($E-I^*$) results in complete inhibition, and the rate constant is represented as k_4 .

One striking observation made in this study is that the association rate and binding affinity of plasmin with C-terminally truncated α_2 -antiplasmin (P414stop) were relatively high ($k_{a1} = 5.1 \times 10^5 M^{-1} s^{-1}$; $K_D = 49$ nM). It is important to note that surface plasmon resonance studies were performed with active site-blocked plasmin, suggesting that the rapid association and high affinity observed in the absence of the C-terminal extension were mediated by exosite interactions between α_2 -antiplasmin and the plasmin protease domain. These important interactions between the α_2 -antiplasmin core domain, outside the immediate vicinity of P1-P1', and the

active site cleft of plasmin are also likely to contribute specificity to the serpin/protease interaction. Having additional exosite interactions is not uncommon in the serpin inhibition mechanism, as it may aid in the recognition of its target protein (18, 19). Together with the specific binding of the α_2 -antiplasmin C terminus to plasmin kringle domains, this leads to an exquisite specificity of the interaction minimizing off-target inhibition of non-cognate proteases.

In summary, we have performed detailed kinetic and binding studies of the interaction between α_2 -antiplasmin and plasmin. Within the α_2 -antiplasmin C terminus, we have measured the contribution of the conserved lysines to the interaction with the plasmin kringle domains. This study demonstrates that the C-terminal lysine (Lys-464) is the single most important amino acid in this domain. The remaining conserved lysine residues within the C terminus of α_2 -antiplasmin individually contribute less, but together significantly enhance the rate of association of serpin with plasmin. These data support the zipper model of interaction whereby Lys-464 binds initially to plasmin (most likely at K1), followed by progressive binding of the other conserved lysines (Lys-448, Lys-441, and Lys-434) to the remaining lysine-binding kringle domains (K4, K5, and K2) (6). Our data also highlight the importance of exosite interactions between the α_2 -antiplasmin core serpin and the plasmin

α_2 -Antiplasmin Binding to Plasmin

protease domain, which provide an additional mechanism of specificity in the serpin/protease interaction.

Acknowledgments—We thank Drs. Elizabeth Gardiner and Ping Fu for advice and guidance in setting up surface plasmon resonance experiments.

REFERENCES

1. Lijnen, H. R. (2001) *Ann. N.Y. Acad. Sci.* **936**, 226–236
2. Matsuno, H. (2006) *Curr. Pharm. Des.* **12**, 841–847
3. Gross, P. L., and Weitz, J. I. (2009) *Clin. Pharmacol. Ther.* **86**, 139–146
4. Lee, K. N., Lee, C. S., Tae, W. C., Jackson, K. W., Christiansen, V. J., and McKee, P. A. (2000) *J. Biol. Chem.* **275**, 37382–37389
5. Coughlin, P. B. (2005) *FEBS J.* **272**, 4852–4857
6. Frank, P. S., Douglas, J. T., Locher, M., Llinás, M., and Schaller, J. (2003) *Biochemistry* **42**, 1078–1085
7. Clemmensen, I., Thorsen, S., Müllertz, S., and Petersen, L. C. (1981) *Eur. J. Biochem.* **120**, 105–112
8. Law, R. H., Sofian, T., Kan, W. T., Horvath, A. J., Hitchen, C. R., Langendorf, C. G., Buckle, A. M., Whisstock, J. C., and Coughlin, P. B. (2008) *Blood* **111**, 2049–2052
9. Hortin, G. L., Gibson, B. L., and Fok, K. F. (1988) *Biochem. Biophys. Res. Commun.* **155**, 591–596
10. Gerber, S. S., Lejon, S., Locher, M., and Schaller, J. (2010) *Cell. Mol. Life Sci.* **67**, 1505–1518
11. Wang, H., Yu, A., Wiman, B., and Pap, S. (2003) *Eur. J. Biochem.* **270**, 2023–2029
12. Morris, E. C., Dafforn, T. R., Forsyth, S. L., Missen, M. A., Horvath, A. J., Hampson, L., Hampson, I. N., Currie, G., Carrell, R. W., and Coughlin, P. B. (2003) *Biochem. J.* **371**, 165–173
13. Horvath, A. J., Irving, J. A., Rossjohn, J., Law, R. H., Bottomley, S. P., Quinsey, N. S., Pike, R. N., Coughlin, P. B., and Whisstock, J. C. (2005) *J. Biol. Chem.* **280**, 43168–43178
14. Schechter, N. M., and Plotnick, M. I. (2004) *Methods* **32**, 159–168
15. Morton, T. A., Myszka, D. G., and Chaiken, I. M. (1995) *Anal. Biochem.* **227**, 176–185
16. Shieh, B. H., and Travis, J. (1987) *J. Biol. Chem.* **262**, 6055–6059
17. Christensen, U., Bangert, K., and Thorsen, S. (1996) *FEBS Lett.* **387**, 58–62
18. Whisstock, J. C., Silverman, G. A., Bird, P. I., Bottomley, S. P., Kaiserman, D., Luke, C. J., Pak, S. C., Reichhart, J. M., and Huntington, J. A. (2010) *J. Biol. Chem.* **285**, 24307–24312
19. Lin, Z., Jiang, L., Yuan, C., Jensen, J. K., Zhang, X., Luo, Z., Furie, B. C., Furie, B., Andreasen, P. A., and Huang, M. (2011) *J. Biol. Chem.* **286**, 7027–7032